# Evidence for functional and non-functional classes of peptides translated from long non-coding RNAs

Jorge Ruiz-Orera[1,*], Pol Verdaguer-Grau[2], José Luis Villanueva-Cañas[1], Xavier Messeguer[2], M.Mar Albà[1,3,*]

[1]Evolutionary Genomics Group, Research Programme on Biomedical Informatics, Hospital del Mar Research Institute, Universitat Pompeu Fabra, Barcelona, Spain; [2]Computer Sciences Department, Universitat Politècnica de Catalunya, Barcelona, Spain; [3]Catalan Institution for Research and Advanced Studies, Barcelona, Spain.

*To whom correspondence should be addressed.

Running title: pervasive translation

Keywords: ribosome profiling, translation, de novo gene, long non-coding RNA, peptide, polymorphism, natural selection

## Abstract

There is accumulating evidence that some genes have originated *de novo* from previously non-coding genomic sequences. However, the processes underlying *de novo* gene birth are still enigmatic. In particular, the appearance of a new functional protein seems highly improbable unless there is already a pool of neutrally evolving peptides that can at some point acquire new functions. Here we show for the first time that such peptides do not only exist but that they are prevalent among the translation products of mouse genes that lack homologues in rat and human. The data suggests that the translation of these peptides is due to the chance occurrence of open reading frames with a favorable codon composition. Our approach combines ribosome profiling experiments, proteomics data and non-synonymous and synonymous nucleotide polymorphism analysis. We propose that effectively neutral processes involving the expression of thousands of transcripts all the way down to proteins provide a basis for *de novo* gene evolution.

The mammalian genome is pervasively transcribed, this includes functional genes but also thousands of transcripts that are not conserved across species and which show weak or no signatures of natural selection[1–3]. Many of the latter transcripts are annotated as long non-coding RNAs (lncRNAs) because they lack conserved long open reading frames (ORFs). Recent studies based on the sequencing of ribosome-protected RNA fragments (ribosome profiling) have reported that a surprisingly large fraction of these transcripts is likely to translate small peptides[4–9], although the significance of this finding has remained elusive.

Each ribosome profiling experiment generates millions of ribosome footprints that are subsequently mapped to the genome or the transcriptome to identify open reading frames (ORFs) that are being translated[10]. The codon-by-codon movement of the ribosome along the coding sequence results in a characteristic pattern of three nucleotide periodicity of the mapped reads, which makes ribosome profiling a very useful method to detect novel events of translation[4,11,12]. Given enough sequence coverage the technique can uncover low-abundant small peptides that would be otherwise difficult to detect by standard proteomics approaches[13,14].

To assess the functional relevance of novel events of translation one can use the ratio between the number of non-synonymous and synonymous substitutions in the putative coding sequences[4,5]. However, this method requires an alignment of at least two homologous sequences. A more general approach that can be used in the absence of homology is the ratio between the number of non-synonymous and synonymous single nucleotide polymorphisms, compared to the one expected under neutrality. Under no selection, non-synonymous and synonymous polymorphisms accumulate at the same rate, whereas under purifying selection there is a deficit of non-synonymous polymorphisms because some amino acid changes disrupt the protein's function[15]. Single nucleotide polymorphism analysis can be performed on a gene-by-gene basis or in pools of sequences that share certain features[2,16].

We previously observed that, as a whole, putatively translated lncRNAs and young protein-coding genes share a number of similarities, such as small ORF size and weak selective

45 constraints, compared with more widely conserved genes[8]. This pointed to a link between the
46 translation of lncRNAs and the evolution of new proteins, but it did not solve the key question of
47 whether translation of new ORFs could occur in the absence of selection at the protein level.
48 This is a fundamental issue because for a new protein to acquire a function it first needs to be
49 produced in the cell at significant amounts. Here by employing a combination of ribosome
50 profiling data, sequence analysis and single nucleotide polymorphism information we obtain
51 strong evidence that the majority of mouse proteins that are not conserved in rat or human
52 selection evolve in a neutral manner. This study renders visible for the first time a layer of
53 protein expression that is not dependent on selective processes, filling a gap in our
54 understanding of the processes underlying *de novo* gene birth.
55

56 **Results**

57

58 First we set to identify translated open reading frames (ORFs) in mouse protein-coding genes
59 (codRNAs) and long non-coding RNAs (lncRNAs) using ribosome-profiling RNA-sequencing
60 (Ribo-Seq) data from eight different tissues and cell lines (Supplementary Table 1 and
61 references therein). In contrast to RNA sequencing (RNA-Seq) reads, which are expected to
62 cover the complete transcript, Ribo-Seq reads correspond to regions bound by ribosomes. We
63 mapped the RNA-Seq and Ribo-Seq reads to the mouse Ensembl gene annotations and, for the
64 sake of completeness, also to a set of previously obtained novel mouse transcripts that did not
65 correspond to annotated genes[3].

66 We used the RibORF program[4] to identify *bona fide* translated sequences among ORFs
67 covered by at least 10 Ribo-Seq reads in transcripts expressed in one or more tissues (Fig. 1a
68 and Supplementary Table 1). This program calculates a score for each ORF depending on the
69 3-nucleotide periodicity and uniformity of the mapped reads. Using a highly stringent RibORF
70 score cut-off of 0.7[4] we found that about 90% of the coding genes (15,020), and 20% of the
71 annotated lncRNAs (539), were predicted to be translated in at least one sample. Additionally,
72 we identified 286 genes that did not map to the gene annotations but contained translated
73 ORFs (Fig. 1b). A widely used criterion to annotate a transcript as protein-coding is the

74 presence of an ORF encoding a protein of at least 100 amino acids[17]. Not surprisingly, the vast
75 majority of ORFs translated from annotated and novel lncRNAs encoded proteins smaller than
76 100 amino acids (smORFs).

77 We hypothesized that some of the translated ORFs may evolve in a neutral manner and
78 constitute a reservoir for the evolution of new protein-coding genes. To test this hypothesis, we
79 first identified translated ORFs that were mouse-specific and then tested them for signatures of
80 selection. We performed exhaustive sequence similarity searches of the ORFs against high
81 coverage transcriptomes from human and rat as well as against the annotated proteomes of
82 101 different eukaryotic species (Fig. 2a, Supplementary Table 2 for a list of species, see
83 Methods for more details). For these searches we discarded any proteins shorter than 24 amino
84 acids, as the detection of homologues may be compromised in such cases due to lack of
85 sufficient sequence information. We identified 1,980 different translated ORFs that showed no
86 homology to expressed sequences in other species (class non-conserved or NC). In general,
87 these ORFs had lower codon usage bias than conserved ORFs, as measured by a previously
88 described hexamer-based coding score metric[8] (Fig. 2b).
89
90 To measure the strength of selection in conserved and non-conserved translated ORFs we
91 employed a large collection of mouse single nucleotide polymorphisms (SNPs) for the house
92 mouse subspecies *Mus musculus castaneus* [18]. We could map a total of 324,729 SNPs to the
93 set of translated ORFs. We grouped the ORFs into three different classes on the basis of
94 conservation and coding score (Fig. 2b), and calculated the ratio between the number of
95 observed non-synonymous and synonymous SNPs (PN/PS(obs)) in each class. We then
96 normalized it by the same ratio expected under neutrality (PN/PS(exp)). The expected PN/PS
97 was estimated using a table of nucleotide mutation frequencies in *Mus musculus castaneus* and
98 the observed codon frequencies in each set of sequences of interest (Supplementary Tables 3
99 and 4). This allowed us not only to compare the strength of selection across different sets of
100 sequences, as done in a previous study of ORFs translated from lncRNAs[8], but also to discard
101 selection if the normalized PN/PS was not significantly different from 1. Specifically, we used a
102 chi-square test that compared the number of observed and expected non-synonymous and
103 synonymous SNPs in each sequence set (Supplementary Table 5). As expected, the PN/PS of

104 randomly selected ORFs from introns was approximately 1. Instead, the PN/PS of conserved
105 ORFs was around 0.15 (Fig. 2c, chi-square test p-value < $10^{-5}$), consistent with protein
106 functionality. One example in this group was Stannin[19,20], a highly conserved peptide that
107 regulates neuronal cell apoptosis (Fig. 3).
108
109 Non-conserved ORFs with high coding scores (NC-H coding score ≥ 0.1014, Fig. 2b and c,
110 Supplementary Figure 1) had weak but significant signatures of selection (p-value < 0.05),
111 possibly because of the existence of some functional mouse-specific genes. In contrast, the
112 PN/PS ratio of the remaining non-conserved ORFs was not significantly different from 1,
113 consistent with neutral evolution. Very similar results were obtained for non-conserved genes
114 annotated as coding or lncRNA (Fig. 2c) and the two sets were merged into a single group of
115 neutrally evolving ORFs (neutral ORFs). This set comprised about two thirds of the non-
116 conserved ORFs (1,291 out of 1,980 ORFs analysed), and represented ~6.8% of the total
117 number of mouse translated ORFs.
118
119 We used proteomics data from the PRIDE database[21] to further validate the translation of this
120 latter group of proteins. Despite their small size (median 44 amino acids), a limiting factor for
121 their detection by standard proteomics-based tecniques[22], we found proteomics evidence for 32
122 of the neutral ORFs (see Methods). This represents 2.5% of the proteins in this set (compared
123 to less than 0.2% false positive rate, see Methods). This fraction is similar to the one obtained
124 for conserved proteins subsampled to have a similar size distribution as the neutral ORFs
125 (2.9%; in contrast, about 41% of all conserved ORFs have proteomics evidence). The test
126 based on the PN/PS ratio confirmed that this subset of 32 ORFs did not deviate significantly
127 from neutrality either (Supplementary Table 5).
128
129 The above analyses grouped the sequences into classes before computing the PN/PS ratio. In
130 general, ORF-by-ORF analysis was not possible because the ORFs were small and contained
131 too few SNPs. Nevertheless, 41 of the neutrally evolving ORFs contained 10 or more SNPs,
132 and we decided to compute a normalized PN/PS ratio for these individual cases. The median
133 PN/PS of these ORFs was around 1 and the distribution of PN/PS values was very different

134 from that of conserved ORFs (Fig. 2d, Wilcoxon test, p-value < $10^{-5}$), consistent with the
135 previous results. Finally, we quantified the number of ORFs that contained SNPs that generated
136 premature stop codons, truncating more than half of the ORF, in the set of neutrally evolving
137 ORFs and in the set of conserved ORFs. In the first case we found 72 out of 1,282 ORFs that
138 contained this type of mutation (5.6%) and in the second case 296 out of 16,892 ORFs (1.75%).
139 Considering that neutral ORFs are in general much shorter than conserved ORFs (median
140 protein size 44 *versus* 412 amino acids), and thus less likely to accumulate ORF-truncating
141 mutations by chance alone, the data clearly indicates a strong excess of ORF-truncating SNPs
142 in neutral ORFs with respect to conserved ORFs. These analyses further support that the
143 selective pressures acting on both kinds of ORFs are very different.
144
145 We next inspected in more detail the ribosome profiling patterns of neutral ORFs with respect to
146 the rest of translated ORFs (hereafter called "functional"). Genes with a recent origin are usually
147 expressed at lower levels than older genes[23,24,3], so it was not surprising to observe that
148 neutrally evolving ORFs were associated with a lower number of Ribo-Seq reads per base than
149 the rest of translated ORFs (median 0.193 versus 0.474, respectively, Supplementary figure 2).
150 Consistent with translation, read periodicity in both neutral and functional ORFs was much
151 higher than the random expectation of 0.33 (median values 0.70 and 0.80, respectively; see
152 examples in Figure 3). Importantly, the results were highly reproducible across tissues (Figure
153 4a for hippocampus and embryonic stem cells; Supplementary Figure 3 hippocampus and
154 brain), a result we would not expect in the case of spurious ribosome profiling signals. In
155 general, the RibORF score of the translated ORFs was positively related to the number of
156 mapped Ribo-Seq reads (Spearman correlation R=0.408), and to the size of the ORFs
157 (Spearman correlation R=0.193). When we controlled for these two parameters, neutral and
158 functional ORFs had equivalent distributions of RibORF score, periodicity and uniformity values
159 (Figure 4b).
160
161 Subsequently, we compared our results to those obtained with two negative controls. The first
162 control contained ORFs in alternative frames of annotated protein coding sequences with
163 experimental protein evidence ("off-frame"). The second one contained randomly occurring

164 ORFs in small nuclear and nucleolar annotated RNA sequences ("sRNA"). The latter RNAs are
165 sometimes detected in ribosome profiling experiments due to the formation of ribonucleoprotein
166 particles that protect the RNA from degradation[25]. As before, we only considered ORFs with at
167 least 10 Ribo-Seq mapped reads. As expected, the vast majority of the ORFs in these controls
168 did not display significant 3-nucleotide read periodicity (Supplementary figure 2, see a specific
169 example in Figure 3). We found that only 234 out of 13,596 ORFs in "off-frame", and 10 out of
170 304 ORFs in "sRNA", had a RibORF score ≥0.7 (the threshold employed throughout our study).
171 This corresponds to an overall false discovery rate (FDR) of 1.75%, much lower than the
172 fraction of neutrally evolving proteins detected in our main analysis (6.8%).
173
174 Some transcripts contained relatively long ORFs but were not translated. One example of this
175 sort was the previously described *de novo* non-coding gene *Poldi*[26] that lacked any evidence of
176 translation in the data we analysed. We next asked which factors may influence the translation
177 of some neutrally evolving ORFs but not of others. First, we inspected the translation initiation
178 sequence context but did not detect any significant differences between translated and non-
179 translated ORFs (Supplementary Figure 4). We then hypothesized that the ORF coding score
180 could affect the "translatability" of the transcript because codons that are abundant in coding
181 sequences are expected to be more efficiently translated than other codons. Consistent with
182 this hypothesis, we found that the translated neutrally evolving ORFs exhibited higher coding
183 scores than non-translated ORFs with otherwise similar characteristics (Fig. 5a, Translated
184 versus non-translated Wilcoxon test, p-value < $10^{-5}$). Importantly, we obtained a similar result
185 after controlling for gene expression level (Fig. 5b, Wilcoxon test, p-value < $10^{-5}$). This is
186 consistent with codon composition having an effect *per se* in ORF translation. When controlling
187 by coding score, expression level, but not ORF length, had an effect on the translatability of the
188 transcript (Fig. 5c).
189
190 The results suggest that the neutral ORFs that are translated are enriched in codons that are
191 frequently found in functional protein coding sequences. This is consistent with the observation
192 that abundant codons enhance translation elongation[27], whereas rare codons might affect the
193 stability of the mRNA[28]. It has been previously hypothesized that the distinction between

194 translated and non-translated lncRNAs may be related to the relative amount of the lncRNA in
195 the nucleus and the cytoplasm[4]. However, we found evidence that some lncRNAs with nuclear
196 functions, such as *Malat1* and *Neat1*, were translated, suggesting that the cytosolic fraction of a
197 transcript can be translated independently of its role or preferred location.
198
199
200 **DISCUSSION**
201
202 The molecular mechanisms underlying *de novo* gene evolution are still poorly understood[29,30,31].
203 The sudden appearance of a new protein-coding gene from a genomic segment seems *a priori*
204 highly improbable, but the process becomes much more likely if the genome is already being
205 pervasively transcribed and translated outside functional protein-coding genes. An excess of
206 transcription was already noted in the first large-scale cDNA sequencing efforts performed in
207 human and mouse[32], and more recent studies have found a high rate of transcriptional turnover
208 when comparing closely related species[33]. Here we have shown that many of these transcripts
209 are translated even if they only contain small ORFs, with the data currently available we have
210 been able to identify 1,291 peptides in 1,132 genes that are likely to be of recent evolutionary
211 origin and that show no signs of selection. This number is likely to be a gross underestimate
212 because many transcripts are expressed at low levels, limiting their detection, and many cell
213 types and tissues have not yet been sampled. According to recent estimates, the cost of
214 transcription and translation in multicellular organisms is probably too small to overcome genetic
215 drift[34]. Therefore, these activities may be effectively neutral. Our results indeed support that
216 there is no barrier for the production of peptides that do not confer an immediate selective
217 advantage.
218
219 The putative precursors of novel proteins identified here are of small size, which is consistent
220 with observations for functional *de novo* genes identified in previous studies[23,35–37]. We have
221 also shown that random ORFs with a more favorable, coding-like, hexamer composition are
222 more likely to be translated than other ORFs. Codon usage bias in functional sequences is
223 related to the abundance of different tRNAs and correlates with expression level[38,39]. Thus, it

224 seems logical that the translated neutral ORFs are biased towards those codons that are
225 translated more efficiently.
226
227 The process of *de novo* gene origination involves the gain of a useful function by a previously
228 non-functional sequence. The rate at which this happens remains to be determined but it has
229 been observed that many random peptide sequences can function as secretion signals[40], and
230 selection for ATP-binding activity in a library of randomly generated 80 amino acid polypeptides
231 successfully identified several candidates capable of binding to ATP[41]. Recent experiments
232 performed in *E.coli* also suggest that random sequences can often affect cellular growth[42]. The
233 pervasive translation of the transcriptome implies that *de novo* gene evolution has much more
234 material at its disposal than previously thought.
235
236
237 **METHODS**
238
239 **Transcript assembly**
240
241 We used strand-specific polyA+ RNA sequencing data (RNA-Seq) data from different mouse
242 and human tissues to assembly the species transcriptomes (Gene Expression Omnibus mouse
243 GSE69241[3], GSE43721[43], and GSE43520[44]; human GSE69241[3]). The mouse RNA samples
244 were extracted from strain Balb/C. RNA-Seq reads were filtered by length (> 25 nucleotides)
245 and by quality using Condetri (v.2.2)[45] with the following settings: -hq = 30 –lq = 10. We aligned
246 the reads to the corresponding reference species genome with Tophat (v. 2.0.8, –N 3, -a 5 and
247 –m 1)[46]. Multiple mapping to several locations in the genome was allowed unless otherwise
248 stated. We assembled the transcriptome with Stringtie[47], merging the reads from all the
249 samples, with parameters -f 0.01, and -M 0.2. We used the species transcriptome as a guide
250 (Ensembl v.75), including all annotated isoforms, but permitting the assembly of annotated and
251 novel isoforms and genes (antisense, intergenic and intronic) as well. We excluded lncRNAs
252 that overlapped annotated pseudogenes or that showed significant sequence similarity to
253 known protein-coding sequences (BLASTP, e-value < $10^{-4}$). In the case of rat we employed a

254 previously generated transcript assembly[48].

255

256 **Ribosome profiling data**

257

258 We used ribosome profiling data (Ribo-Seq) from 8 different mouse tissues or cell lines (see
259 Supplementary Table 1), obtained from Gene Expression Omnibus under accession numbers
260 GSE51424[49], GSE50983[50], GSE22001[51], GSE62134[52], GSE72064[53], and GSE41246. Only
261 datasets corresponding to non-pathogenic conditions were considered. The reads from the
262 experimental replicates were merged before using RibORF to increase the resolution of the
263 read periodicity, as done in the original RibORF paper[4]. For all analyses we considered only
264 genes expressed at significant levels in at least one sample (RNA-Seq fragments per kilobase
265 per Million mapped reads (FPKM) > 0.2). The expression of the genes detected in these
266 samples is expected to be highly representative of the *Mus musculus* species as a whole. We
267 mapped several brain RNA-Seq datasets from *Mus musculus castaneus*[33] to the mouse
268 assembled transcriptome using NextGenMap[54]. As expected, the vast majority of the genes
269 expressed in brain samples from C57BL/6 mice[49] also showed evidence of expression in *Mus*
270 *musculus castaneus* brain RNA samples[33](Supplementary Table 6).

271

272 We discarded anomalous reads (length < 26 or > 33 nt) and reads that mapped to annotated
273 rRNAs and tRNAs in mouse from the Ribo-Seq sequencing datasets. Next, reads were mapped
274 to the assembled mouse genome (mm10) with Bowtie (v. 0.12.7, parameters -k 1 -m 20 -n 1 --
275 best --strata). Considering that the ORFs had to be extensively covered by reads to be
276 considered translated (high uniformity), we decided to include multiple mapped reads so as not
277 to compromise the detection of paralogous proteins (Supplementary Fig. 7). We used the
278 mapping of the Ribo-Seq reads to the complete set of annotated coding sequences in mouse to
279 compute the position of the P-site (second binding site for tRNA in the ribosome) for reads of
280 different size, as previously described[10,12].

281

282 **Identification of translated ORFs**

283

284 We predicted all translated ORFs (ATG to STOP) with a minimum length of 9 amino acids in the
285 transcripts with RibORF (v.0.1)[4]. Only ORFs with a minimum of 10 mapped Ribo-Seq reads
286 were considered. The RibORF classifier is based on a support vector machine algorithm,
287 originally applied to human transcripts. The input parameters are the read periodicity and the
288 read uniformity. The first one is the fraction of reads that correspond to the correct frame and
289 the second one corresponds to the percentage of maximum entropy, a value of 1 indicates a
290 completely even distribution of reads. For each ORF the program computes a score that
291 depends on the values of these two parameters[4]. We used the same score cut-off as in the
292 original paper (≥ 0.7), which had a reported false positive rate of 0.67% and false negative rate
293 of 2.5%.
294
295 We eliminated any redundancy in the translated ORFs by taking the longest ORF when several
296 overlapping translated ORFs were detected in the same gene. The identification of translated
297 ORFs was done separately for the different tissues (Supplementary Table 1), and the data was
298 subsequently integrated, taking the tissue with the highest RibORF score as representative.
299 Differences in the number of translated ORFs in different tissues were related to the depth of
300 sequencing and the number of reads that mapped to the top 5 most highly expressed proteins
301 (Supplementary Fig. 6 and 7, respectively). For genes with no evidence of translation we
302 selected the longest ORF across all transcripts for comparative purposes. Selecting the longest
303 ORF was justified by the fact that, in translated ORFs, the ORF with the highest number of
304 mapped Ribo-Seq reads was usually the longest ORF (75.7% for codRNAs and 84% for
305 lncRNAs). We also generated a set of 4,013 randomly taken ORFs from introns, after discarding
306 ORFs that showed significant sequence similarity to known proteins from the same species
307 (BLASTP, e-value < $10^{-4}$).
308
309 We generated a negative control set by combining out-of-frame ORFs in mouse coding genes
310 with experimental protein evidence according to Uniprot ("off-frame") and randomly occurring
311 ORFs in mouse small nuclear and nucleolar RNAs ("sRNAs"). These ORFs were required to
312 have at least 10 Ribo-Seq mapped reads and were processed in the same manner as the main
313 set of ORFs under study. The total number of sequences in the negative control was 13,900.

314 We also generated a positive control set composed of 2,163 randomly taken annotated mouse
315 coding sequences with protein evidence in Uniprot. With these controls we estimated a false
316 positive rate of 1.75% and a false negative rate of 2.54% for the above mentioned RibORF
317 score cut-off.
318
319 **Sequence conservation**
320
321 We searched for mouse translated ORF homologues in the human and rat transcriptomes using
322 TBLASTN (limited to one strand, e-value < $10^{-4}$)[55]. We also performed sequence similarity
323 searches against the annotated proteomes of 67 mammalian-species and 34 non-mammalian
324 eukaryotes from a diverse range of groups compiled in a previous study[48], using BLASTP (e-
325 value < $10^{-4}$). For these searches we only considered query proteins of size 24 amino acids or
326 longer, as shorter proteins may not contain sufficient information to perform homology searches.
327 Mouse ORFs that did not have any homology hits in other species were classified as non-
328 conserved, the rest as conserved. Translated non-conserved ORFs located upstream or
329 downstream of another longer ORF in a conserved transcript (uORFs and dORFs) were
330 excluded from this analysis.
331
332 We inspected the rat genomic syntenic regions of translated ORFs using LiftOver[56]. We
333 classified the ORFs in two groups depending on whether the ORF was truncated in rat or not
334 (the truncation had to affect more than half of the protein). For neutrally evolving ORFs the
335 number of cases in which the ORF was truncated was similar to the number of cases in which it
336 was not truncated, and in both cases the polymorphism patterns were consistent with neutrality
337 (Supplementary Table 5). This indicated that, for this group, the presence of a similar ORF in rat
338 does not imply functional conservation of the ORF. Therefore, we did not use information on rat
339 genomic synteny to classify the genes as conserved/non-conserved.
340
341 **Single nucleotide polymorphism analysis**
342
343 We obtained single nucleotide polymorphism (SNP) data from 20 individuals of the house

344 mouse subspecies *Mus musculus castaneus*[18]. We classified SNPs in ORFs as non-
345 synonymous (PN, amino acid altering) and synonymous (PS, not amino-acid altering). We
346 calculated the PN/PS ratio in each ORF group by using the sum of PN and PS in all the
347 sequences ((PN/PS)obs). We calculated the expected PN/PS under neutrality ((PN/PS)exp)
348 using the mutation frequencies between pairs of nucleotides in *Mus musculus castaneus* and
349 the codon composition of the different sequences or sets of sequences under study
350 (Supplementary Tables 2 to 5). The observed transition to transversion ratio was 4.42, very
351 similar to the 4.26 value obtained in early observations based on mouse-rat divergence data[57].
352 We tested for purifying selection by the number of observed and expected non-synonymous
353 and synonymous SNPs using a chi-square test with one degree of freedom. Positively selected
354 mutations are rapidly fixed in the population and their effect is expected to be negligible when
355 using SNP data.
356
357 **Proteomics data**
358
359 We used the proteomics database PRIDE[21] to search for peptide matches in the proteins
360 encoded by various gene sets. For a protein to have proteomics evidence, we required at least
361 two distinct perfect matches of peptides that did not map to any other protein in the dataset,
362 allowing for up to two mismatches. These are very stringent conditions with a false positive rate
363 < 0.2%[48].
364
365 **Coding score**
366
367 We used a previously described metric based on hexamer frequencies to calculate the coding
368 score of the sequences[8]. The method uses a table of pre-calculated hexamer scores that
369 measure the relative frequency of each hexamer in coding versus non-coding sequences.
370 These scores are then used to evaluate the coding propensity of a sequence based on its
371 hexamer composition. The method has been implemented in a computational program called
372 CIPHER that can be accessed online (http:// http://evolutionarygenomics.upf.edu/cipher).
373

374 **Statistical tests and plots**

375

376 The generation of plots and statistical tests was performed with the R package[58].

377

378 **Data availability**

379

380 Transcript assemblies from mouse, human and rat, as well as the mouse open reading frames
381 (ORFs) predicted to be translated have been deposited at figshare
382 (http://dx.doi.org/10.6084/m9.figshare.4702375). The code and executable file to calculate the
383 coding score can be accessed at https://github.com/jorruior/CIPHER.
384 The C program to calculated the PN/PS expected under neutrality is available at
385 https://figshare.com/articles/computePNPS_c/5085706. Supplementary file 1 contains
386 supplementary tables and figures.

387

**REFERENCES**


388 1. Kutter, C. *et al.* Rapid turnover of long noncoding RNAs and the evolution of gene
389 expression. *PLoS Genet.* **8,** e1002841 (2012).
390 2. Wiberg, R. A. W. *et al.* Assessing Recent Selection and Functionality at Long Noncoding
391 RNA Loci in the Mouse Genome. *Genome Biol. Evol.* **7,** 2432–44 (2015).
392 3. Ruiz-Orera, J. *et al.* Origins of De Novo Genes in Human and Chimpanzee. *PLOS*
393 *Genet.* **11,** e1005721 (2015).
394 4. Ji, Z., Song, R., Regev, A. & Struhl, K. Many lncRNAs, 5'UTRs, and pseudogenes are
395 translated and some are likely to express functional proteins. *Elife* **4,** e08890 (2015).
396 5. Raj, A. *et al.* Thousands of novel translated open reading frames in humans inferred by
397 ribosome footprint profiling. *Elife* **5,** (2016).
398 6. Ingolia, N. T., Lareau, L. F. & Weissman, J. S. Ribosome profiling of mouse embryonic
399 stem cells reveals the complexity and dynamics of mammalian proteomes. *Cell* **147,**
400 789–802 (2011).
401 7. Ingolia, N. T. *et al.* Ribosome Profiling Reveals Pervasive Translation Outside of

402 Annotated Protein-Coding Genes. *Cell Rep.* **8,** 1365–79 (2014).
403 8. Ruiz-Orera, J., Messeguer, X., Subirana, J. A. & Alba, M. M. Long non-coding RNAs as
404 a source of new peptides. *Elife* **3,** e03523 (2014).
405 9. Wilson, B. A. & Masel, J. Putatively noncoding transcripts show extensive association
406 with ribosomes. *Genome Biol. Evol.* **3,** 1245–52 (2011).
407 10. Ingolia, N. T., Ghaemmaghami, S., Newman, J. R. S. & Weissman, J. S. Genome-wide
408 analysis in vivo of translation with nucleotide resolution using ribosome profiling. *Science*
409 **324,** 218–23 (2009).
410 11. Bazzini, A. A. *et al.* Identification of small ORFs in vertebrates using ribosome
411 footprinting and evolutionary conservation. *EMBO J.* **33,** 981–93 (2014).
412 12. Calviello, L. *et al.* Detecting actively translated open reading frames in ribosome profiling
413 data. *Nat Meth* **13,** 165–170 (2016).
414 13. Aspden, J. L. *et al.* Extensive translation of small ORFs revealed by Poly-Ribo-Seq. *Elife*
415 e03528 (2014). doi:10.7554/eLife.03528
416 14. Mackowiak, S. D. *et al.* Extensive identification and analysis of conserved small ORFs in
417 animals. *Genome Biol.* **16,** 1–21 (2015).
418 15. Sunyaev, S., Kondrashov, F. A., Bork, P. & Ramensky, V. Impact of selection, mutation
419 rate and genetic drift on human genetic variation. *Hum. Mol. Genet.* **12,** 3325–3330
420 (2003).
421 16. Gayà-Vidal, M. & Albà, M. M. Uncovering adaptive evolution in the human lineage. *BMC*
422 *Genomics* **15,** 599 (2014).
423 17. Dinger, M. E., Pang, K. C., Mercer, T. R. & Mattick, J. S. Differentiating protein-coding
424 and noncoding RNA: challenges and ambiguities. *PLoS Comput. Biol.* **4,** e1000176
425 (2008).
426 18. Harr, B. *et al.* Genomic resources for wild populations of the house mouse, Mus
427 musculus and its close relative Mus spretus. *Sci. Data* **3,** 160075 (2016).
428 19. Buck-Koehntop, B. A., Mascioni, A., Buffy, J. J. & Veglia, G. Structure, dynamics, and
429 membrane topology of stannin: a mediator of neuronal cell apoptosis induced by
430 trimethyltin chloride. *J. Mol. Biol.* **354,** 652–65 (2005).
431 20. Pueyo, J. I. *et al.* Hemotin, a Regulator of Phagocytosis Encoded by a Small ORF and

432 Conserved across Metazoans. *PLoS Biol* **14,** e1002395 (2016).
433 21. Vizcaíno, J. A. *et al.* 2016 update of the PRIDE database and its related tools. *Nucleic*
434 *Acids Res.* **44,** D447–D456 (2016).
435 22. Slavoff, S. A. *et al.* Peptidomic discovery of short open reading frame-encoded peptides
436 in human cells. *Nat. Chem. Biol.* **9,** 59–64 (2013).
437 23. Toll-Riera, M. *et al.* Origin of primate orphan genes: a comparative genomics approach.
438 *Mol. Biol. Evol.* **26,** 603–12 (2009).
439 24. Xie, C. *et al.* Hominoid-specific de novo protein-coding genes originating from long non-
440 coding RNAs. *PLoS Genet.* **8,** e1002942 (2012).
441 25. Ji, Z., Song, R., Huang, H., Regev, A. & Struhl, K. Transcriptome-scale RNase-
442 footprinting of RNA-protein complexes. *Nat. Biotechnol.* **34,** 410–413 (2016).
443 26. Heinen, T. J. A. J., Staubach, F., Häming, D. & Tautz, D. Emergence of a new gene from
444 an intergenic region. *Curr. Biol.* **19,** 1527–31 (2009).
445 27. Yu, C. *et al.* Codon Usage Influences the Local Rate of Translation Elongation to
446 Regulate Co-translational Protein Folding. *Mol. Cell* **59,** 744–754 (2015).
447 28. Presnyak, V. *et al.* Codon optimality is a major determinant of mRNA stability. *Cell* **160,**
448 1111–24 (2015).
449 29. Tautz, D. & Domazet-Lošo, T. The evolutionary origin of orphan genes. *Nat. Rev. Genet.*
450 **12,** 692–702 (2011).
451 30. Schlötterer, C. Genes from scratch – the evolutionary fate of de novo genes. *Trends*
452 *Genet.* (2015). doi:10.1016/j.tig.2015.02.007
453 31. McLysaght, A. & Hurst, L. D. Open questions in the study of de novo genes: what, how
454 and why. *Nat. Rev. Genet.* **17,** 567–578 (2016).
455 32. Okazaki, Y. *et al.* Analysis of the mouse transcriptome based on functional annotation of
456 60,770 full-length cDNAs. *Nature* **420,** 563–73 (2002).
457 33. Neme, R. & Tautz, D. Fast turnover of genome transcription across evolutionary time
458 exposes entire non-coding DNA to de novo gene emergence. *Elife* **5,** (2016).
459 34. Lynch, M. & Marinov, G. K. The bioenergetic costs of a gene. *Proc. Natl. Acad. Sci. U. S.*
460 *A.* **112,** 15690–5 (2015).
461 35. Carvunis, A.-R. *et al.* Proto-genes and de novo gene birth. *Nature* **487,** 370–4 (2012).

462 36. Zhao, L., Saelao, P., Jones, C. D. & Begun, D. J. Origin and spread of de novo genes in
463 Drosophila melanogaster populations. *Science* **343,** 769–72 (2014).
464 37. Wilson, B. A., Foy, S. G., Neme, R. & Masel, J. Young Genes are Highly Disordered as
465 Predicted by the Preadaptation Hypothesis of De Novo Gene Birth. *Nat. Ecol. Evol.* **1,**
466 0146–146 (2017).
467 38. Plotkin, J. B. & Kudla, G. Synonymous but not the same: the causes and consequences
468 of codon bias. *Nat. Rev. Genet.* (2011). doi:10.1038/nrg2899
469 39. Dana, A. & Tuller, T. The effect of tRNA levels on decoding times of mRNA codons.
470 *Nucleic Acids Res.* **42,** 9171–81 (2014).
471 40. Kaiser, C. A., Preuss, D., Grisafi, P. & Botstein, D. Many random sequences functionally
472 replace the secretion signal sequence of yeast invertase. *Science* **235,** 312–7 (1987).
473 41. Keefe, A. D. & Szostak, J. W. Functional proteins from a random-sequence library.
474 *Nature* **410,** 715–718 (2001).
475 42. Neme, R., Amador, C., Yildirim, B., McConnell, E. & Tautz, D. Random sequences are
476 an abundant source of bioactive RNAs or peptides. *Nat. Ecol. Evol.* (2017).
477 doi:10.1038/s41559-017-0127
478 43. Soumillon, M. *et al.* Cellular source and mechanisms of high transcriptome complexity in
479 the mammalian testis. *Cell Rep.* **3,** 2179–90 (2013).
480 44. Necsulea, A. *et al.* The evolution of lncRNA repertoires and expression patterns in
481 tetrapods. *Nature* **505,** 635–40 (2014).
482 45. Smeds, L. & Künstner, A. ConDeTri--a content dependent read trimmer for Illumina data.
483 *PLoS One* **6,** e26314 (2011).
484 46. Kim, D. *et al.* TopHat2: accurate alignment of transcriptomes in the presence of
485 insertions, deletions and gene fusions. *Genome Biol.* **14,** R36 (2013).
486 47. Pertea, M. *et al.* StringTie enables improved reconstruction of a transcriptome from
487 RNA-seq reads. *Nat Biotech* **33,** 290–295 (2015).
488 48. Luis Villanueva-Cañas, J. *et al.* New Genes and Functional Innovation in Mammals.
489 *Genome Biol. Evol.* **9,** 1886–1900 (2017).
490 49. Gonzalez, C. *et al.* Ribosome profiling reveals a cell-type-specific translational landscape
491 in brain tumors. *J. Neurosci.* **34,** 10924–36 (2014).

492 50. Castañeda, J. *et al.* Reduced pachytene piRNAs and translation underlie spermiogenic
493 arrest in Maelstrom mutant mice. *EMBO J.* **33,** 1999–2019 (2014).
494 51. Guo, H., Ingolia, N. T., Weissman, J. S. & Bartel, D. P. Mammalian microRNAs
495 predominantly act to decrease target mRNA levels. *Nature* **466,** 835–40 (2010).
496 52. Diaz-Munoz, M. D. *et al.* The RNA-binding protein HuR is essential for the B cell
497 antibody response. *Nat Immunol* **16,** 415–425 (2015).
498 53. Cho, J. *et al.* Multiple repressive mechanisms in the hippocampus during memory
499 formation. *Science* **350,** 82–87 (2015).
500 54. Sedlazeck, F. J., Rescheneder, P. & von Haeseler, A. NextGenMap: fast and accurate
501 read mapping in highly polymorphic genomes. *Bioinformatics* **29,** 2790–2791 (2013).
502 55. Altschul, S. F. *et al.* Gapped BLAST and PSI-BLAST: a new generation of protein
503 database search programs. *Nucleic Acids Res.* **25,** 3389–402 (1997).
504 56. Karolchik, D. *et al.* The UCSC Genome Browser database: 2014 update. *Nucleic Acids*
505 *Res.* **42,** D764–D770 (2014).
506 57. Rosenberg, M. S., Subramanian, S. & Kumar, S. Patterns of Transitional Mutation
507 Biases Within and Among Mammalian Genomes. *Mol. Biol. Evol.* **20,** 988–993 (2003).
508 58. R Development Core Team. R: a language and environment for statistical computing.
509 (2016).
510
511 **ACKNOWLEDGEMENTS**
512
513 We are grateful for valuable discussions with many colleagues during this study. The work was
514 funded by grants BFU2012-36820 and BFU2015-65235-P from Ministerio de Economía e
515 Innovación (Spanish Government) and co-funded by FEDER (EC). We also received funding
516 from Agència de Gestió d'Ajuts Universitaris i de Recerca Generalitat de Catalunya (AGAUR),
517 grant number 2014SGR1121.
518
519 **FIGURE LEGENDS**
520
521 **Figure 1. Detection of translated ORFs. a.** Workflow to identify translated ORFs. Ribosome profiling

522 (Ribo-Seq) reads, corresponding to ribosome-protected fragments, are mapped to all predicted canonical
523 ORFs with length ≥ 30 nucleotides in transcripts. This is performed with single-nucleotide resolution after
524 computing the read P-site per each read length. In each ORF, reads per frame and read uniformity are
525 evaluated by RiboORF. **b.** Number of translated and non-translated expressed genes belonging to
526 different classes after integrating data from eight different mouse tissues (Supplementary Table 1). **c.**
527 Number of translated ORFs belonging to different classes. The translated ORFs have been divided into
528 small ORFs (smORF, < 100 aa) and long ORFs (≥ 100 aa), depending on their length.
529
530 **Figure 2. Identification of selection signatures. a**. Workflow to identify conserved and non-conserved
531 ORFs. Translated ORFs shorter than 24 amino acids, as well as non-conserved upstream and
532 downstream ORF in conserved transcripts (uORFs and dORFs, see Methods), were filtered out. Any ORF
533 with at least one BLAST match in another species was classified as conserved (C), otherwise it was
534 classified as non-conserved (NC). **b.** Coding score in conserved (C) and non-conserved ORFs (NC).
535 Conserved ORFs showed significantly higher coding score values than non-conserved ones; *** Wilcoxon
536 test, p-value < $10^{-5}$. Non-conserved ORFs with a high coding score value (≥ 0.1014) were classified as
537 NC-H, and the rest were classified as NC-L. **c**. Analysis of selective constraints in translated ORFs. PN/PS
538 (obs/exp) refers to the normalized ratio between non-synonymous (PN) and synonymous (PS) single
539 nucleotide polymorphisms; a value of 1 is expected in the absence of selection at the protein level.
540 Conserved and NC-H ORFs showed significant purifying selection signatures. In contrast, NC-L ORFs did
541 not show evidence of purifying selection at the protein level. Many conserved ORFs in lncRNAs are likely
542 to encode functional micropeptides. Differences between observed and expected PN/PS were assessed
543 with a chi-square test, * p- value < 0.05, *** p-value < $10^{-5}$. Error bars indicate the standard error of the
544 sample proportion. Numbers of ORFs for the different categories are also displayed. **d.** Distribution of
545 normalized PN/PS values for individual ORFs in different gene classes. Only ORFs with at least 10 SNPs
546 were considered; the NC-H group contained too few cases to be analysed. The differences between C and
547 NC-L are significant (Wilcoxon test, p-value <$10^{-5}$).
548
549 **Figure 3. Three nucleotide periodicity of translated ORFs.** The mapping of Ribo-Seq reads on different
550 types of ORFs is shown. The Y axis represents the log-number of reads, the X axis the positions in the
551 ORF. The reads show strong frame bias in the functional (conserved) and the neutral (NC-L) examples,
552 with a preponderance of in-frame reads (green) versus off-frame reads (red and blue), while the frame bias
553 is randomly distributed in the negative control (SNORA18). The exon/intron structure and the amino acid
554 sequence for translated ORFs is also shown.
555

556 **Figure 4. Properties of neutrally evolving ORFs. a.** Relationship between the percentage of reads
557 falling in the correct frame in neural embryonic stem cells cells and hippocampus samples, for neutral and
558 functional ORFs having at least 10 reads in both samples and being translated in at least one sample.
559 Spearman correlation coefficient is R=0.4224 for the neutrat set (p-value < $10^{-5}$) and R=0.4360 for the
560 functional set (p-value < $10^{-5}$). **b.** Distribution of read periodicity, read uniformity and RibORF scores in
561 neutral and functional translated ORFs after controlling for the number of Ribo-Seq reads and size of
562 ORFs. The 'functional normalized' set is a randomly taken subset of the functional ORFs that has the
563 same number of mapped Ribo-Seq reads and ORF size distribution as the set of neutrally evolving ORFs
564 (n=900). Data is represented as box-plots for different number of read intervals; the box contains 50% of
565 the data, horizontal line is the median value.
566
567 **Figure 5. Factors influencing the translation of neutrally evolving ORFs. a.** Influence of coding score
568 in the translatability of neutrally evolving ORFs. Translated ORFs showed significantly higher coding score
569 than non-translated ORFs, both sets had significantly higher coding scores than introns (Wilcoxon test p-
570 value < $10^{-5}$, indicated by ***). **b.** Influence of coding score in the translatability of ORFs controlling for
571 gene expression values, the two sets have comparable maximum FPKM gene expression (median FPKM
572 value = 11.10). Translated ORFs showed significantly higher coding score values than non-translated
573 ORFs; (Wilcoxon test p-value < $10^{-5}$). **c.** Influence of maximum FPKM gene expression and ORF length in
574 the translatability of neutral ORFs normalized by coding score (median coding score value = -0.0052).
575 Translated ORFs showed significantly higher FPKM values than non-translated ORFs (Wilcoxon test p-
576 value < $10^{-5}$); differences in length were not significant.
577

578 **FIGURES**

579 **Figure 1**

580

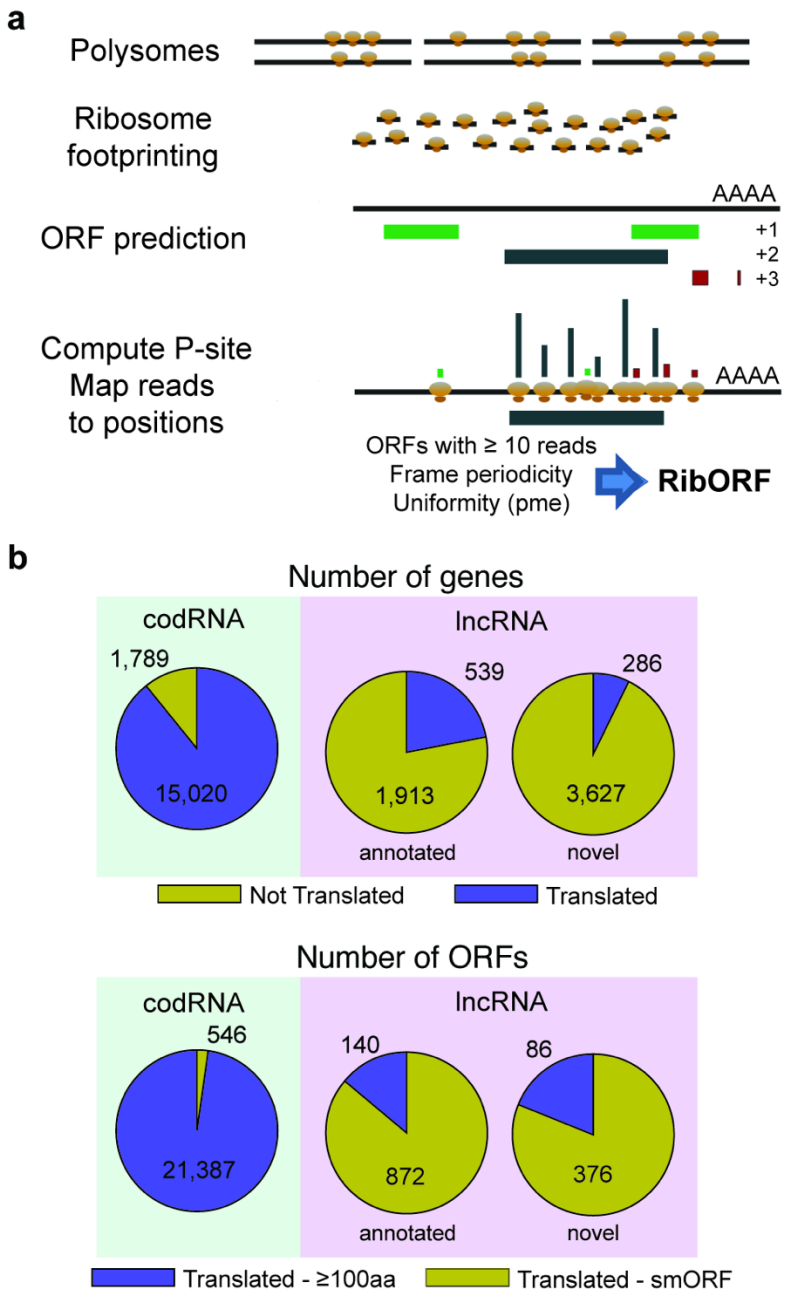


581

582

583 **Figure 2**

584

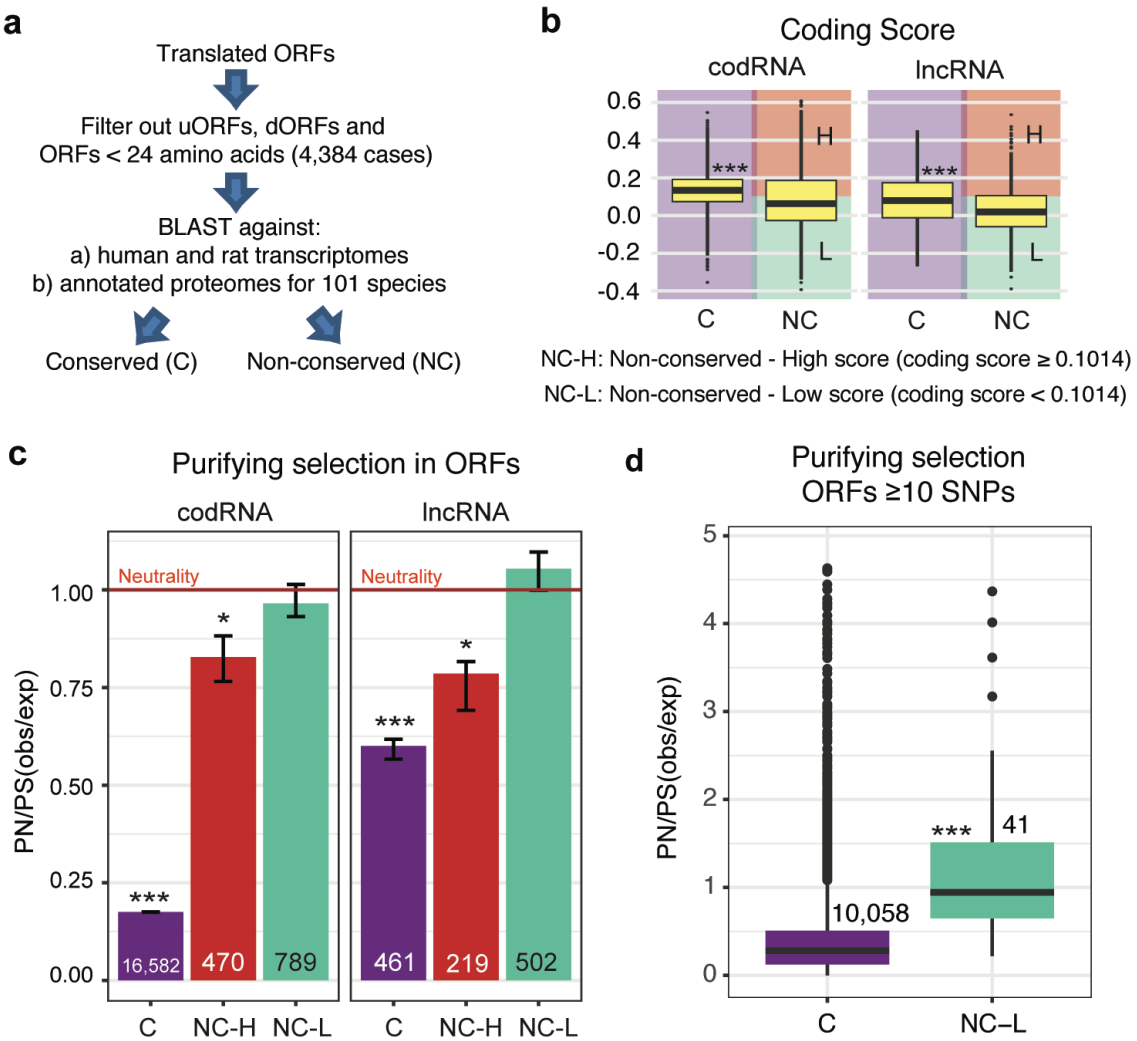


585

586

587 **Figure 3**

588

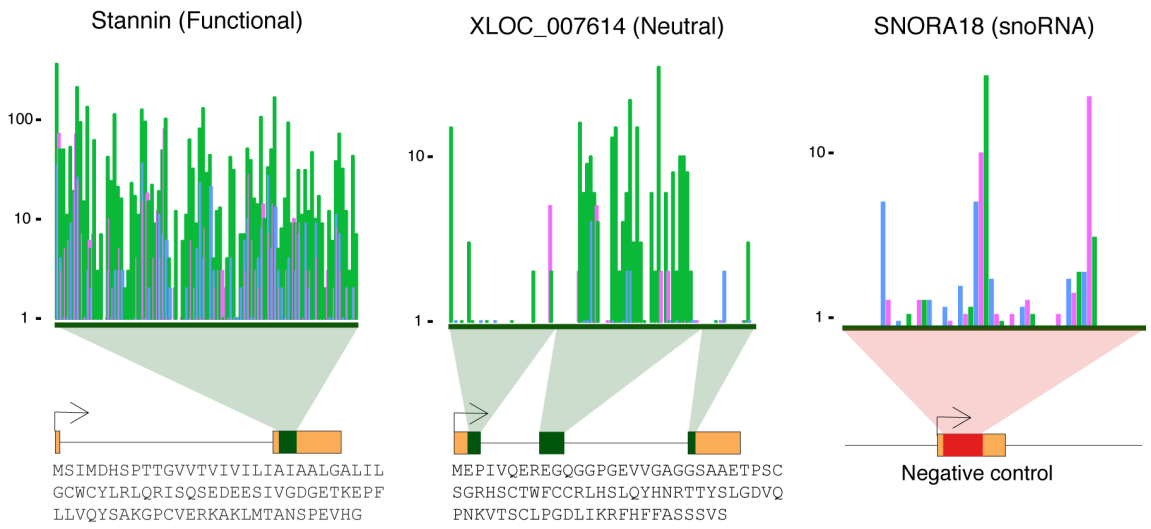


589

590

591 **Figure 4**

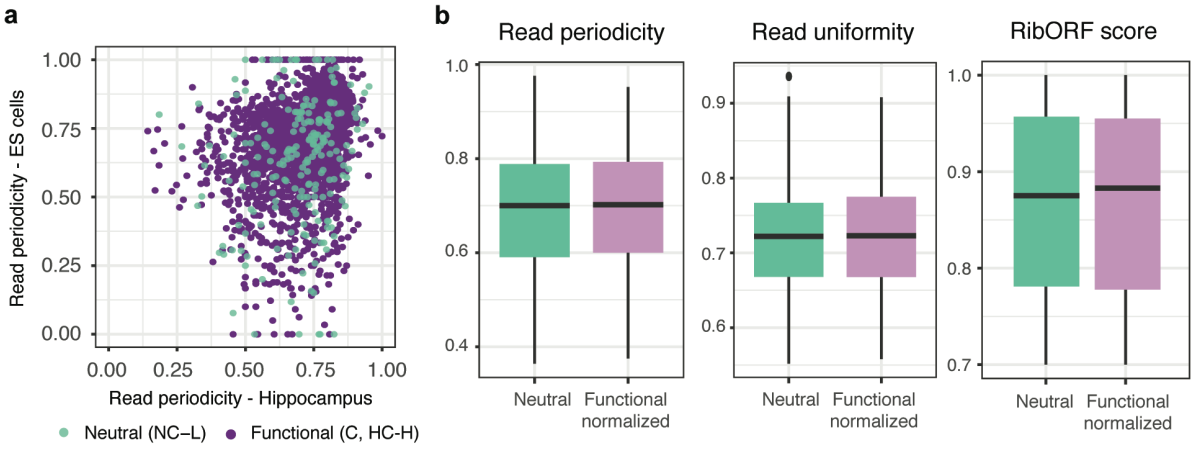


592

593

**Figure 5**

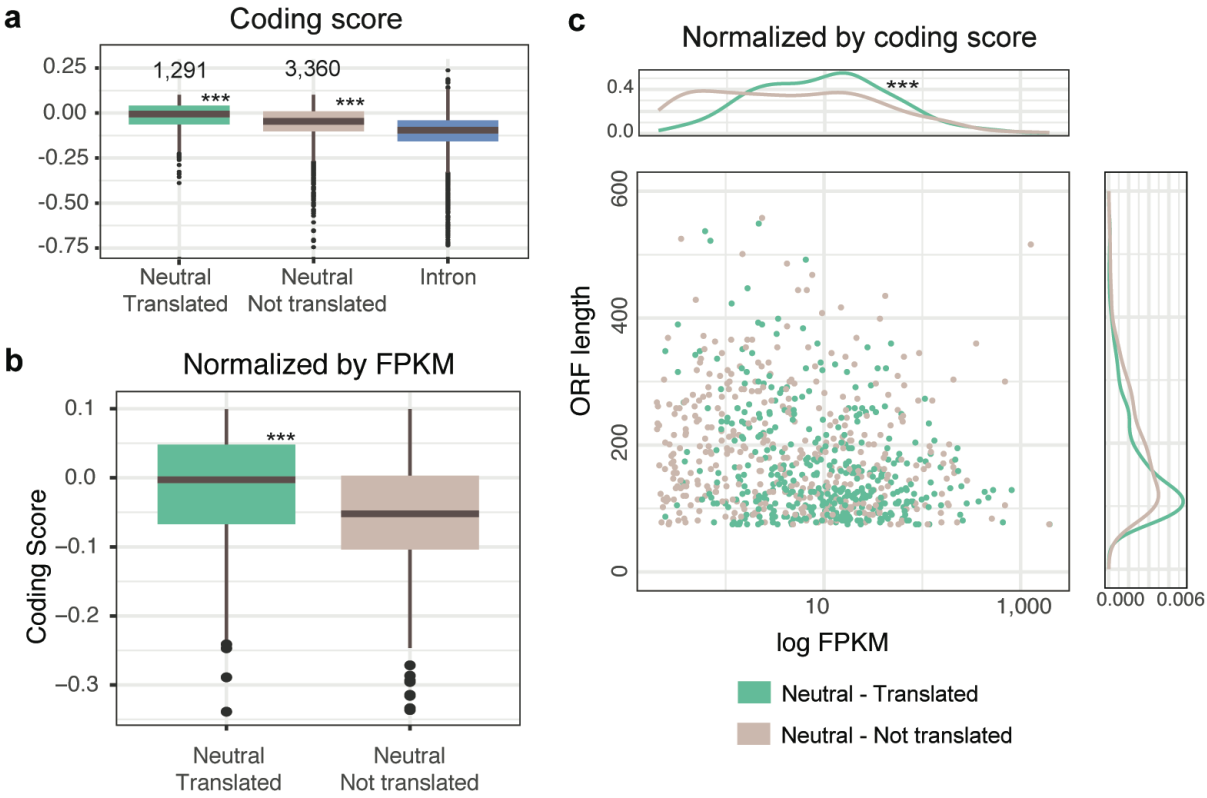
a
Coding score
0.25
0.00
-0.25
-0.50
-0.75
1,291
3,360
***
***
Neutral Translated
Neutral Not translated
Intron
b
Normalized by FPKM
Coding Score
0.1
0.0
−0.1
−0.2
−0.3
***
Neutral Translated
Neutral Not translated
c
Normalized by coding score
0.4
0.0
***
ORF length
600
400
200
0
10
1,000
log FPKM
0.000
0.006
Neutral - Translated
Neutral - Not translated